Macromolecules

Article

pubs.acs.org/Macromolecules

Amphiphilic BODIPY-Based Photoswitchable Fluorescent Polymeric Nanoparticles for Rewritable Patterning and Dual-Color Cell Imaging

Jian Chen,*[,†,‡] Weibang Zhong,[†] Ying Tang,[‡] Zhan Wu,[‡] Ya Li,[†] Pinggui Yi,*[,†] and Jianhui Jiang*[,‡]

[†]Key Laboratory of Theoretical Organic Chemistry and Functional Molecule of Ministry of Education, Hunan University of Science and Technology, Xiangtan 411201, P. R. China

[‡]State Key Laboratory of Chemo/Biosensing and Chemometrics, Hunan University, Changsha 410082, P. R. China

Supporting Information

ABSTRACT: Photoswitchable fluorescent polymeric nanoparticles (PFPNs) with controllable molecular weight, high contrast, biocompatibility, and prominent photostability are highly desirable but still scarce for rewritable printing, super-resolution bioimaging, and rewritable data storage. In this study, novel amphiphilic BODIPY-based PFPNs with considerable merits are first synthesized by a facile one-pot RAFT-mediated miniemulsion polymerization method. The polymerization is performed by adopting polymerizable BODIPY and spiropyran derivatives, together with MMA as monomer, and mediated by utilizing biocompatible PEO macro-RAFT agent as both control agent and reactive stabilizer. The amphiphilic BODIPY-based PFPNs not only exhibit reversibly photoswitchable fluorescence properties under the alternative UV and visible light illumination through induced intraparticle fluorescence resonance energy transfer (FRET) but also display controllable molecular weight with narrow polydispersity index (PDI), high contrast of fluorescence, tunable energy transfer efficiency, good biocompatibility, excellent photostability, favorable photoreversibility, etc. The as-prepared PFPNs are successfully demonstrated for rewritable fluorescence patterning and high-contrast dual-color fluorescence imaging of living cells, implying its potential for rewritable data storage and broad biological applications in cell biology and diagnostics.

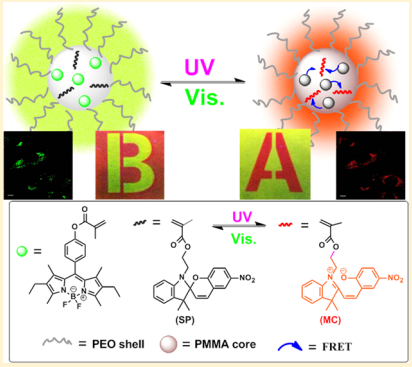

INTRODUCTION

The successful preparation of photoswitchable fluorescent nanoparticles (PFNs) has been extensively studied for their potential applications as chemical sensing, rewritable data storage, and ultrahigh-resolution biological imaging.[1] In general, PFNs often utilize photochromic compounds, such as spiropyrans,[2] diarylethenes,[3] and spirooxazines,[4] to bring photoswitchable fluorescence property. In a popular fluorescence resonance energy transfer (FRET) strategy, these photochromes, like spiropyrans,[2] usually act as switchable energy acceptors under the irradiation of UV or visible light to quench or recover the fluorescence of another nearby energy-matched fluorophores (energy donor). Obviously, these are the desired features which help to overcome the autofluorescence interference of cells in bioimaging or surpass the limitation of spatial resolution of ~250 nm for routine fluorescence microscopy.[1a,5]

To date, various strategies such as surface modification,[6] self-assembly method,[7] and microemulsion[2a,b] or miniemulsion polymerization,[8] etc., have been employed to prepare various PFNs. However, it is noteworthy that the surface modification of fluorescent nanoparticles like quantum dots has potential defects such as blinking and cytotoxicity,[9] and the self-assembly strategy often involves a complicated synthesis,[7] while the adoption of microemulsion polymerization is hard to modulate the amount of embedded dyes,[2a,b] which is ascribed to the different diffusion coefficients between the selected dyes with monomer or matrix in water (or another media). In addition, many reported PFNs often introduced fluorescent dyes via doping or physical adsorption, which implies potential dye leakage and aggregation, significantly limiting their advanced biological applications.[2d,8c] Notably, although traditional miniemulsion polymerization has displayed some advantages for preparing PFNs, such as facile and versatile preparation route, improved photostability, and tunable amount of incorporated dyes,[8] there are still some problems like surfactant migration or desorption need to be resolved, when adopting general ionic surfactant like sodium dodecyl sulfate (SDS).[10] In addition, the radical polymerization process in conventional miniemulsion strategy also cannot control the polymerization rate and the polydispersity index (PDI) of formed polymer, which will be bring undesirable effects on the architecture of prepared polymers or the morphology of particles.[10] To overcome these drawbacks, a facile and elegant way is to adopt reversible addition−fragmentation chain transfer (RAFT)-mediated miniemulsion polymerization strategy and use amphiphilic macromolecular (macro-) RAFT agents as both stabilizer and control agent.[11] These macro-RAFT agents

Received: March 30, 2015
Revised: May 4, 2015

DOI: 10.1021/acs.macromol.5b00667
Macromolecules XXXX, XXX, XXX−XXX

can induce the *in situ* generation of block copolymers with controllable molecular weight and a predictably narrow PDI[11] as well as form the final stable amphiphilic particles. However, to the best of our knowledge, there is little information about using macro-RAFT agents and RAFT-mediated miniemulsion polymerization to fabricate PFNs.

On the other hand, as a well-known fluorescent dye, BODIPY derivatives have exhibited high brightness and tunable emission spectrum.[12] Thus, they can be selected as ideal candidates to fabricate various photoswitchable fluorescence systems.[4b,13] However, there is no report about introducing BODIPY derivatives into nanoparticles to prepared novel PFNs; most of the reported BODIPY-based photoswitchable fluorescence systems are based on organic compounds which often involve complicate synthetic pathway and cannot be directly used in water due to their hydrophobic nature.[4b,13] Obviously, these drawbacks strongly limit their potential applications in the super-resolution imaging of biological samples.

Herein, we reported the first preparation of novel amphiphilic BODIPY-based photoswitchable fluorescent polymeric nanoparticles (PFPNs) in aqueous media via an one-pot RAFT-mediated miniemulsion polymerization, with a biocompatible poly(ethylene oxide) (PEO) macro-RAFT agent (PEO-TTC, Scheme S1) as both control agent and reactive stabilizer. This novel strategy undoubtedly endows as-prepared PFPNs with controllable molecular weight and narrow PDI, improved stabilization, and biocompatibility. Moreover, in this study, two hydrophobic dyes as BODIPY methacrylate (BDPMA) and spiropyran-linked methacrylate (SPMA) were covalently linked to the polymer backbone with tunable amount and ratio, which can not only greatly increase the photostability of as-prepared PFPNs but also significantly improve their brightness and photoswitch contrast in water. In addition, these novel amphiphilic PFPNs also reveal other advantages, such as controllable FRET efficiency, improved long-term photostability, and favorable photoreversibility, etc. More importantly, the novel PFPNs can be directly applied in rewritable fluorescence patterning and high-contrast dual-color fluorescence imaging of living cells, which implies the great potential in rewritable data storage and biological diagnosis.

EXPERIMENTAL SECTION

Materials. Poly(ethylene glycol) methyl ether (PEO-OH, M_w = 1900, Alfa), *N*,*N*′-dicyclohexylcarbodiimide (DCC, 99%, Alfa), 4-(dimethylamino)pyridine (DMAP, 99%, Alfa), *n*-hexadecane (HD, 99%, Aldrich), 2,4-dimethyl-3-ethylpyrrole (97%, Aldrich), boron trifluoride diethyl etherate (2 M in diethyl ether, Aldrich), 4-hydroxybenzaldehyde (98%, Aldrich), tetrachloro-1,4-benzoquinone (Chloranil, 99%, Aldrich), *N*,*N*-diisopropylethylamine (DIPEA, 99.5%, Aldrich), trifluoroacetic acid (TFA, 99%, Aldrich), and 2-(3′,3′-dimethyl-6-nitrospiro[chromene-2,2′-indolin]-1′-yl)ethanol (SP-OH, 93%, TCI) were used as received. Methyl methacrylate (MMA, 99%, Aldrich) was washed with 10% sodium hydroxide solution and deionized water for three times and then purified by vacuum distillation. 2,2′-Azobis(isobutyronitrile) (AIBN, 99.99%, Aldrich) was recrystallized from ethanol. The double-distilled water, which was used throughout this work, was further purified with a Milli-Q system. Tetrahydrofuran (THF, A.R.), dichloromethane (A.R.), and acetonitrile (A.R.) were distilled over CaH_2. Petroleum ether, benzene, and other reagents were analytical reagents and used without further purification. The PEO macro-RAFT agent (PEO-TTC, end-functionality >95%, Scheme S1 and Figure S1)[11] and BODIPY phenol (Scheme S2 and Figure S2)[12] were synthesized as described elsewhere.

Synthesis of BODIPY Methacrylate (BDPMA). BDPMA was synthesized according to modified literature procedures.[12] First, an anhydrous CH_2Cl_2 solution (50 mL) of BODIPY phenol (475 mg, 1.2 mmol), methacrylic acid (309 mg, 3.6 mmol), and DMAP (29 mg, 0.24 mmol) was cooled to 0 °C under a N_2 atmosphere; then, DCC (370 mg, 1.8 mmol) in anhydrous CH_2Cl_2 (5 mL) was slowly added to the opaque solution. The mixture was stirred at room temperature for 24 h. After that the mixture was concentrated and purified by silica gel column chromatography (CH_2Cl_2/petroleum ether = 7:3 v/v), affording 456 mg of BDPMA product (82% yield). ^{1}H NMR (500 MHz, $CDCl_3$, δ): 0.98 (t, 6H, J = 1.0 Hz, CH_3), 1.34 (s, 6H, CH_3), 2.09 (s, 3H, CH_3), 2.30 (q, 4H, CH_2), 2.53 (s, 6H, CH_3), 5.81 (s, 1H, CH), 6.40 (s, 1H, CH), 7.28 (d, 2H, Ar H), 7.33 (d, 2H, Ar H) (Figure S3 of Supporting Information).

Synthesis of Spiropyran-Linked Methacrylate (SPMA). SPMA was synthesized according to modified literature procedures.[2c] An anhydrous CH_2Cl_2 solution (45 mL) of SP-OH (1.00 g, 2.84 mmol), methacrylic acid (1.22 g, 14.20 mmol), and DMAP (0.069 g, 0.57 mmol) was cooled to 0 °C under a N_2 atmosphere and protection against sunlight exposure. Then DCC (0.877g, 4.26 mmol) in anhydrous CH_2Cl_2 (5 mL) was slowly added to the solution over 0.5 h. The mixture was stirred for 24 h at room temperature, and then the mixture was concentrated and purified by silica gel column chromatography (CH_2Cl_2/petroleum ether = 2:1 v/v), affording 950 mg of SPMA product (80% yield). ^{1}H NMR (500 MHz, $CDCl_3$, δ): 1.17 (s, 3H, CH_3), 1.28 (s, 3H, CH_3), 1.92 (s, 3H, CH_3), 3.45−3.54 (m, 2H, CH_2), 4.3 (t, 2H, CH_2), 5.57 and 6.07 (d, 2H, CH_2), 5.87 (d, 1H, CH), 6.71 (q, 2H, Ar H) 6.92 (q, 2H, Ar H), 7.09 (d, 1H, Ar H), 7.17−7.23 (m, 1H, Ar H), 7.96−8.05 (m, 2H, Ar H) (Figure S4 of Supporting Information).

Synthesis of Amphiphilic PFPNs. The organic phase containing MMA, BDPMA, SPMA, hexadecane, and initiator AIBN was added to the aqueous phase (water and PEO-TTC) and stirred for 15 min; then the mixture was ultrasonicated (650 W, JY92-IIN, power 15%) for 15 min. The as-prepared miniemulsion was transferred to a three-necked flask and purged with N_2 for 30 min. The polymerization was performed at 75 °C for 7 h to obtain a stable amphiphilic PFPNs aqueous dispersion. The unreacted monomer or other impurities were removed by dialysis three times through a porous cellulose membrane (MWCO 3500). The detailed experimental parameters for this polymerization are shown in Table 1.

Table 1. Summary of Some Data for BDPMA and SPMA Contained Nanoparticle Samples

sample[a]	BDPMA feed [mg]	SPMA feed [mg]	diameter[b] [nm]	FL intensity[c] [au]
NP-N0	0	0	85	
NP-N1	3	2.5	87	616
NP-N2	3	5	76	600
NP-N3	3	10	77	595
NP-N4	3	15	79	377
NP-S	0	10	91	9

[a]The MMA/HD/PEO-TTC/AIBN feed is 0.5/0.05/0.075/0.006 g, respectively. [b]Average nanoparticle diameter, determined by DLS. [c]Excitation at 500 nm and emission at 550 nm, 25 °C, C_{PFPNs} = 0.3 wt %.

Photorewritable Fluorescence Patterning. Quadrate filter papers were soaked in a MFPNs dispersion (NP-N3, 3 wt %) for 24 h at room temperature and dried via natural seasoning to keep the filter papers cover with MFPNs equably. Photomasks with hollowed out letter "A" or "B" (Figure S8) were designed and fabricated by local advertising design company. Photorewritable fluorescence patterning were achieved by circularly covering/removing masks (A and B) on the filter paper under alternating 302 nm UV and 525 nm visible light illumination.

Cell Culture. CellTiter 96 AQueous One Solution Cell Proliferation Assay was purchased from Promega (Madison, WI).

DOI: 10.1021/acs.macromol.5b00667
Macromolecules XXXX, XXX, XXX−XXX

Scheme 1. Schematic Illustration of Amphiphilic PFPNs via Covalently Combining BODIPY Monomer (BDPMA) and Photochromic Derivative (SPMA)

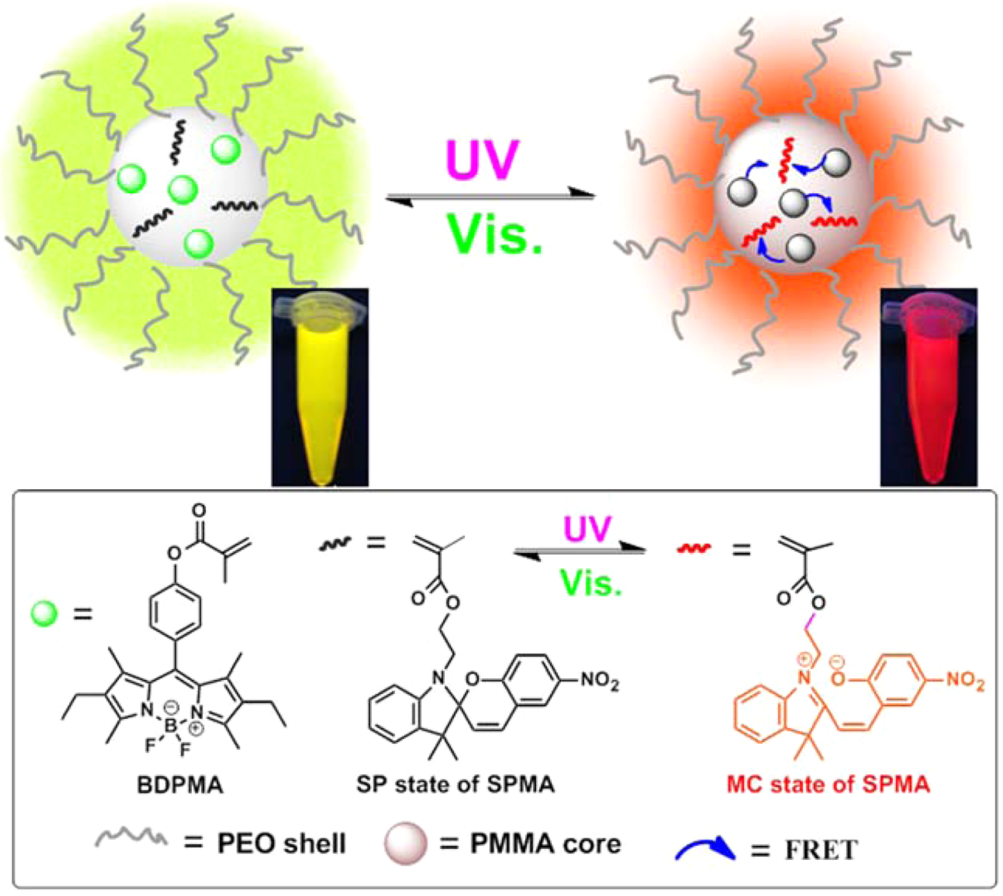

Cell culture media was purchased from Thermo Scientific HyClone (Waltham, MA). A549 cells, which were obtained from the cell bank at Xiangya Hospital (Changsha, China), were cultured in RPMI-1640 medium containing 100 U/mL of penicillin–streptomycin and 10% fetal bovine serum (FBS). The cells were grown at 37 °C in an incubator with a 5% CO_2 humidified atmosphere.

***In Vitro* Cytotoxicity Measurement.** The effect of PFPNs on cell proliferation in A549 cells was performed via the CellTiter 96 AQueous One Solution Cell Proliferation Assay. First, cells were seeded at a density of 5.0×10^3 cells per well in 96-well plates in three replicates and incubated overnight in 200 μL of complete medium. Then, cells were dealt with various diluted samples of PFPNs in the presence of 10% serum. After 24 h of incubation, 96-well plates were washed with cold phosphate buffered saline (PBS) for three times (137 mM NaCl, 2.7 mM KCl, 10 mM Na_2HPO_4, 1.8 mM KH_2PO_4, pH 7.4), then 120 μL of fresh medium containing 20 μL of CellTiter 96 AQueous One Solution was added to every well, and the plate was incubated again for 1 h at 37 °C. Thereafter, the absorbance of each plate was measured via a Thermo Scientific Multiskan MK3Microplate Reader (Thermo Fisher, USA) at 490 nm.

Confocal Imaging. A549 cells were seeded in confocal dishes at a density of ca. 20% per plate and cultured for 24 h at 37 °C. Then, 500 μL of fresh cell growth medium supplemented with PFPNs (100 μg/mL) was added to each dish. After incubation for 3 h, the dishes were washed with cold PBS for three times. Then, A549 cells were incubated with 1 mL of fresh medium for fluorescence imaging. All fluorescence images were acquired using an oil immersion objective (100×, NA 1.3) on an Olympus FV1000 confocal laser scanning fluorescence microscope containing an Olympus IX81 inverted microscope. First, an Ar^+ laser (488 nm) was used as green irradiation source, and a 505–560 nm bandpass filter was used for green fluorescence detection. Then, cell dishes were exposed to a ZF-1 type three ultraviolet analyzer UV lamp (365 nm) for 30 s and used Ar^+ laser (405 nm) as red irradiation source, and a 575–650 nm bandpass filter was used for red fluorescence detection.

Other Measurements. ^{1}H NMR spectra was measured on a Bruker Avance 500 MHz NMR spectrometer. The number-average molecular weight (M_n) and PDI were determined by a Waters 2410 gel permeation chromatograph (GPC) at 30 °C and using THF as the eluent (1.0 mL/min). The calibration curve was obtained by using polystyrene (PS) as the standard. The diameter of nanoparticles was determined by a Malvern Nano-ZS90 instrument, and their morphology was recorded on a Bruker Dimension Icon atomic force microscope (AFM) in the tapping mode. The UV–vis absorption spectrum was measured on a Shimadzu UV-2501PC spectrophotometer at room temperature. The fluorescence spectrum was determined by a Shimadzu RF-5301PC fluorescence spectrophotometer at room temperature. The solid content of nanoparticles was estimated by gravimetric analysis. Fluorescence lifetime (τ) was recorded on a time-correlated single photon counting (TCSPC) nanosecond fluorescence spectrometer (Edinburgh FLS920) at room temperature. For PFPNs, data analysis was carried out by using a simple tail fit method and fitting with a monoexponential decay function. The goodness of fit was estimated by using χ^2 values (between 1.0 and 1.2).

RESULTS AND DISCUSSION

Synthesis of Amphiphilic PFPNs. In this study, novel amphiphilic PFPNs were prepared by an one-pot RAFT-mediated miniemulsion polymerization.[11] In detail, two polymerizable dyes as BDPMA (Figure S3) and SPMA (Figure S4) were copolymerized with MMA in the presence of a PEO macro-RAFT agent (PEO-TTC, Scheme S1 and Figure S1) as

DOI: 10.1021/acs.macromol.5b00667
Macromolecules XXXX, XXX, XXX–XXX

both control agent and reactive nonionic surfactants in miniemulsion. The well-defined amphiphilic nanoparticles with a hydrophobic photoswitchable fluorescent core and a hydrophilic PEO shell were gradually achieved via the generation of PEO-*b*-P(MMA-*co*-BDPMA-*co*-SPMA) diblock copolymers from the hydrophilic PEO-TTC and the *in situ* self-assembly process during the polymerization. Obviously, the copolymerization of fluorescent monomer and photochromic derivative can successfully avoid the potential dye leakage, so as to greatly enhance the structural stability and photostability of the obtained PFPNs. The as-prepared amphiphilic PFPNs dispersion in aqueous media displayed reversibly distinct dual-color fluorescence via alternate illumination of UV and visible light, as illustrated in Scheme 1.

Figure 1 shows the GPC traces of macro-RAFT agent PEO-TTC and PEO-*b*-PMMA copolymer from obtained amphiphilic

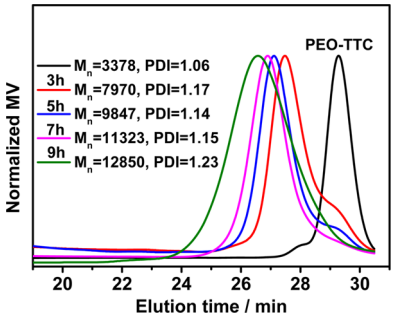

Figure 1. GPC curves of macro-RAFT agent PEO-TTC and the obtained PEO-*b*-PMMA copolymer via one-pot RAFT-miniemulsion polymerization.

polymeric nanoparticles without incorporation of BDPMA and SPMA at different reaction time via typical one-pot RAFT-miniemulsion polymerization. For this experiment, a detailed description is shown in the Supporting Information. As exhibited in Figure 1, with the reaction time increased, GPC trace of the obtained PEO-*b*-PMMA copolymer was gradually shifted to the region of high molecular weight. The M_n and PDI of the synthesized PEO-*b*-PMMA are also displayed in Figure 1. The reaction time increased from 3 to 9 h. As shown in Figure 1, the M_n of PEO-*b*-PMMA gradually increased from 7970 to 12 850 g/mol; meanwhile, the PDI always kept a low value (<1.25), which indicated the typical "living" property of selected RAFT-miniemulsion polymerization technique. Moreover, in current experimental conditions, compared with other reaction times, 7 h seems to be more helpful for us to prepare the well-defined amphiphilic diblock copolymer with relatively high molecular weight and narrow PDI.

Generally, particles with smaller size are affected little by light scattering and display more potential for additional biomodification and biological applications.[14] Herein, the averaged particle diameter ranging from ca. 85 to ca. 129 nm was achieved by modulating some experimental parameters as shown in Table S1, which strongly relied on the concentration of used surfactant, PEO-TTC. For example, as for sample NP-S3, by using 7.5 mg/mL PEO-TTC, a stable particle with diameter down to approximately 85 nm was obtained via measuring by DLS (Table S1). However, if the concentration of surfactant was added to 10 mg/mL, some big particles formed, which induced the increase of both the average diameter and the PDI of particles (NP-S4, Table S1). As the concentration (7.5 mg/mL) of PEO-TTC exceeded its critical micelle concentration (CMC),[15] the micelle nucleation could take place during the polymerization process. However, the adopted hydrophobe (hexadecane) could provide enough osmotic pressure to prevent Ostwald ripening, thus forming a stable miniemulsion.[8b]

Figure 2 shows the AFM image of an amphiphilic PFPN sample NP-N3 (Table 1). The AFM result exhibited the

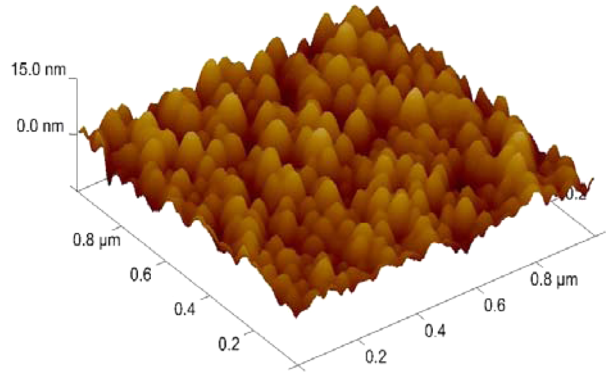

Figure 2. AFM image of amphiphilic PFPNs (sample NP-N3).

presence of well-dispersed global particles with an average diameter of 64 nm. For comparison, the diameter for this sample (NP-N3) measured by DLS is 78 nm (Table 1 and Figure S5). The difference of sizes obtained from AFM and DLS was possibly due to that the AFM scanning was performed on dry solid sample, while the DLS was measured on the unrestricted extension of amphiphilic nanoparticles in aqueous solution. These results indicated that RAFT-mediated miniemulsion polymerization can be used to prepare amphiphilic PFPNs with tunable size.

Spectroscopic Characterization of Amphiphilic PFPNs. Figures 3A and 3B compare the absorption spectra and the fluorescence emission spectra of BDPMA dye in different conditions, including pure water, dichloromethane, and nanoparticles (NP-N3). As a known hydrophobic dye, BDPMA exhibited low absorption (Figure 3A) and negligible fluorescence in water due to its low solubility (Figure 3B).[12] However, it showed intense fluorescence intensity and ultrahigh brightness after it was encapsulated in polymeric nanoparticles.[12] Additionally, the maximum absorption wavelength for BDPMA in nanoparticles sample (NP-N3) and dichloromethane were identical, revealing that the fluorescent dye was located in the hydrophobic polymer matrix.[8c] Notably, inspired by recent G. Clavier's report about copolymerization of BDPMA in polymer nanoparticles, it could be estimated that more than 95% of the feed dyes were covalently linked to the polymer backbone.[12] Furthermore, it is certain that spiropyran derivatives adopt the ring-opened merocyanine (MC) state under UV irradiation, while changing to the ring-closed spiro (SP) state after visible light illumination (Scheme 1).[2,8] As shown in Figure 3A, compared with the visible light irradiation of SPMA-contained samples (NP-N3 and NP-S), a new absorbance band around 570 nm appeared after UV irradiation, which was due to the photoisomerization of the ring-closed SP state to the ring-opened MC state. It demonstrated that the SPMA dyes have also been wonderfully encapsulated in the particles, which is highly consistent with our previously reported results.[8]

DOI: 10.1021/acs.macromol.5b00667
Macromolecules XXXX, XXX, XXX−XXX

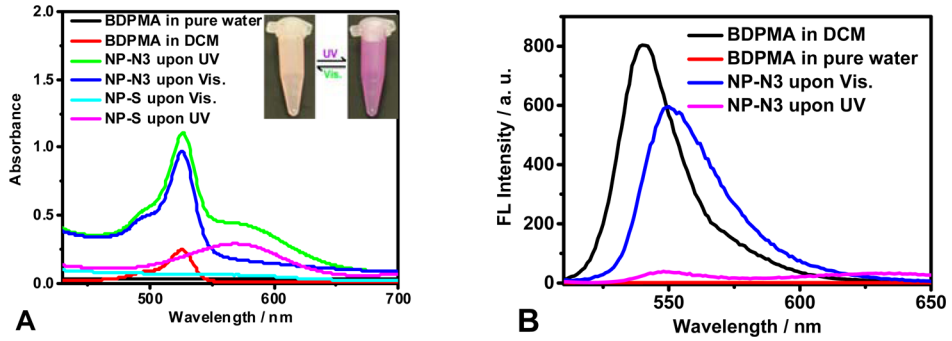

Figure 3. (A) Absorption spectra of BDPMA dye in pure water and dichloromethane, together with a PFPNs sample (NP-N3) and a SPMA contained nanoparticle sample (NP-S) upon UV or visible light. (B) Fluorescence emission spectra of BDPMA dye in pure water and dichloromethane and the PFPNs sample NP-N3 upon UV or visible light (λ_{ex} = 500 nm).

The relationship between the fluorescence intensity and the content of introduced fluorescent dye in nanoparticles is also investigated in this study. For this experiment (Table S1), without changing other experimental conditions, four nanoparticles with different feed amount of BDPMA were designed to compare their fluorescence intensity at the same concentration of particles as shown in Figure S6A,B. With the BDPMA content increasing from 1 to 4 mg in nanoparticles, their maximum absorbance improved correspondingly (Figure S6A), while their fluorescent intensity first increased and then decreased (Figure S6B). Specifically, for the nanoparticle (NP-B4) possesses the highest BDPMA content, its maximum fluorescence intensity is obviously lower than NP-S3, and its fluorescence emission band exhibited a broadened profile with a slightly red-shift (~4 nm) of maximum emission. It means that the possible self-quenching will be induced when the content of fluorophores inside the nanoparticles gets to a certain value.[8] Thus, the proper content of fluorophores in nanoparticles is crucial to provide the nanoparticles with high fluorescence intensity as well as effectively to avoid self-quenching.

Reversibly Photoswitching of PFPNs by UV and Visible Light. Figure 4 compares the change of the

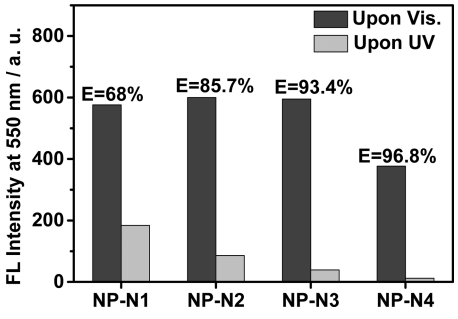

Figure 4. Fluorescence intensity of four PFPNs samples (Table 1) at 550 nm upon UV and visible light irradiation.

fluorescence intensity of four PFPNs samples (Table 1) at 550 nm after irradiating by visible and UV light. As shown in Figure 3B as well as Figures S7 and S8, after illumination of UV light (302 nm) for 3 min, fluorescence emission of all PFPNs samples at 550 nm was dramatically decreased; meanwhile, an emission band around 640 nm appeared (Figure 3B and Figure S7), which remained with the emission band of the MC form of the SPMA units and was consistent with our previous reports.[8] Compared with the intense fluorescence emission of BDPMA moieties in PFPNs at 550 nm, the emission intensity of the MC moieties in PFPNs at 640 nm is relatively weak (Figure 3B and Figure S8) but still can be easily detected via changing the measure condition (Figure S7). We are not sure if the low emission is related to the PMMA matrix.[8] Presumably, the relatively high content of SPMA molecules in nanoparticles was apt to induce fluorescence quenching. After the sample was irradiated again by 10 min of visible light (525 nm), the fluorescence emission at 550 nm was basically recovered, while the emission band around 640 nm disappeared at the same time (Figure 3 and Figure S8). Correspondingly, the luminescence of the PFPNs dispersion in the dark was transparently varied between red and yellow-green after illuminating by UV or visible light, as illustrated in Scheme 1.

According to the principle of FRET,[16] once the emission spectrum of the donor overlaps remarkably with the acceptor's absorption spectrum, and the distance of donor−acceptor resides in the proper radius (ca. 1−10 nm), the FRET between the donor and acceptor is efficient.[16] In the current work, as shown in Figure S9, the emission spectrum of the BDPMA (donor) overlaps wonderfully with the absorption spectrum of the MC state of the SPMA (acceptor) in the PFPNs. In contrast, the absorption spectrum of the SP state of SPMA and the emission spectrum of the BDPMA overlap hardly. Therefore, the FRET from the BDPMA to the SP state of the SPMA is difficult, while the FRET to the MC state is feasible.

As can be seen in Table 2 and Figure 4, for four PFPNs samples (NP-N1 to NP-N4), the estimated average donor−acceptor distances (r) ranged from 3.7 to 5.7 nm, which are similar to some previous reports.[8] And there were multiple acceptors (MC state of SPMA) within the effective energy transfer distance from a donor, which ensured the presence of intraparticle FRET mechanism as well as the photoswitching fluorescence after the irradiation of UV light. As for the sample NP-N1, it has the lowest ratio of acceptor/donor (0.9), and its E is 68.0%; thus, the BDPMA fluorescence cannot be availably decreased after illumination of UV light, while for the higher ratio of acceptor/donor (3.7, NP-N3), there was more MC state of SPMA units around a BDPMA molecule (donor), and quite high E (93.4%) can be obtained. However, E cannot be improved evidently and the initial fluorescence intensity reduced much (Table 1 and Figure S7C), when continue to increase the ratio of acceptor/donor (5.5, NP-N4). Therefore, the optimization of the ratio of acceptor/donor is crucial to achieve ideal PFPNs with sufficient energy transfer efficiency as well as high photoswitch contrast.

DOI: 10.1021/acs.macromol.5b00667
Macromolecules XXXX, XXX, XXX−XXX

Table 2. Characteristics Data of Four PFPNs Samples

sample[a]	D_{NP}[b] [nm]	D_{core}[b] [nm]	N_{BD}[c]	N_{SP}[c]	N_{SP}/N_{BD}	N_A[d]	E[e] [%]	r[f] [nm]
NP-N1	71	68	1358	1253	0.9	3.6	68.0	5.7
NP-N2	62	59	887	1637	1.8	7.3	85.7	4.8
NP-N3	64	61	981	3618	3.7	14.5	93.4	4.2
NP-N4	67	64	1132	6268	5.5	21.8	96.8	3.7

[a]The MMA/HD/PEO-TTC/AIBN feed is 0.5/0.05/0.075/0.006 g, respectively. [b]D_{NP} and D_{core}: the average nanoparticle diameter and core diameter (Supporting Information), obtained by AFM. [c]N_{BD} and N_{SP}: the average number of BDPMA and SPMA in a nanoparticle core, respectively, estimated by presuming more than 90% of dyes are copolymerized. [d]The average number of SPMA residing around one BDPMA within the effective energy transfer distance (Supporting Information). [e]The experimental energy transfer efficiency (Supporting Information). [f]The estimated average donor−acceptor distance (Supporting Information).

To further confirm the presence of intraparticle FRET in current systems, fluorescence decay curves of typical PFPNs sample (NP-N3, Figure 5) after irradiating UV/vis light were

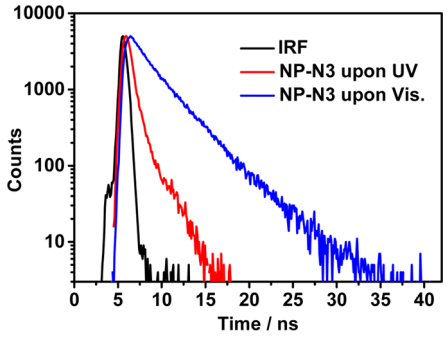

Figure 5. Fluorescence decay curves of NP-N3 upon UV/vis light irradiation (λ_{ex} = 405 nm, detection wavelength = 550 nm).

obtained by using the TCSPC technique.[16] As shown in Figure 5, after illumination of visible light for 10 min (switching on), the selected sample NP-3 displayed a mean lifetime of 2.49 ns, which was similar to previously reported BDPMA-contained polymeric nanoparticles,[12] indicating there is no FRET process between donor and SP state of the SPMA units. After irradiation of UV light for 3 min (switching off), the average lifetime of the PFPNs was significantly reduced to 0.83 ns, which was mainly ascribed to the photoinduced FRET process between donor and acceptor.

Figure 6A displays fluorescence response behavior of the BDPMA-containing nanoparticles sample (NP-S3) and the novel PFPNs sample (NP-N3) under illumination of UV and visible light. During the whole irradiation period of UV (12 W) and visible light (2 W), the fluorescence intensity of BDPMA-containing nanoparticles at 550 nm changed little, which indicated the undetectable photodegradation in such short-time irradiation. In contrast, for the PFPNs sample NP-N3, the fluorescence intensity at 550 nm dramatically decreased within a very short time (3 min) UV irradiation, revealing the FRET between donor and acceptor happened. While its fluorescence intensity can basically recover after irradiation by visible light for 10 min, which can be due to the photoisomerization from MC state to SP state of SPMA units. On the other hand, the fluorescence intensity of as-prepared MFPNs at 550 nm can be reversibly turned on/off via cyclically illuminating UV and visible light (Figure 6B). As revealed in Figure 6B, the photoswitching of fluorescence can be performed for five cycles with a negligible "fatigue" effect. Undoubtedly, the prepared PFPNs with the fluorescent dye and the photochromic incorporated by covalent bonding and protected by a polymer matrix hold superior resistance to the possible "fatigue" effect, as compared to other analogous dyad systems.[13] Moreover, it is worth pointing out that the present PFPNs exhibit a much shorter photoresponse time than some previous systems,[2a,f] which indicated a valuable potential for e.g. rewritable data storage or selective highlighted biological labeling.[2a,e]

In the present study, the fluorescence long-term stability and the thermal stability of MC state of the typical PFPNs sample (NP-N3) were also explored. For the long-term stability test, the diluted dispersion was sealed and stored in the dark under ambient temperature. Then an aliquot was drawn out for fluorescence test after every week. As displayed in Figure 7A, not only the fluorescence intensity but also the photoswitching efficiency of the diluted PFPNs sample changed seldom even after storing for 6 weeks, implying remarkable long-term photostability and the tiny leakage of dyes in PFPNs sample.

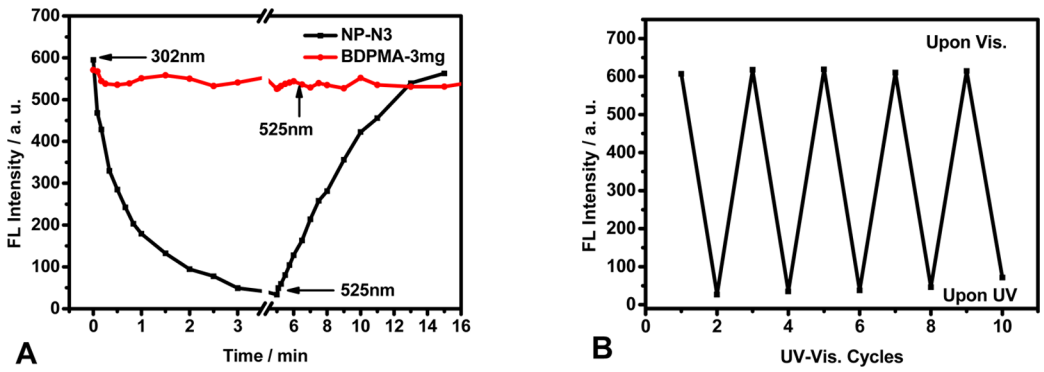

Figure 6. (A) Fluorescence response of BDPMA-contained nanoparticles sample (NP-S3) and a PFPNs sample (NP-N3) via irradiating with UV (302 nm) and visible light (525 nm). (B) Photoinduced switching cycles of a PFPNs sample (NP-3) under alternative illumination of UV for 3 min and visible light for 10 min (C_{PFPNs} = 0.3 wt %, λ_{ex} = 500 nm, λ_{em} = 550 nm).

DOI: 10.1021/acs.macromol.5b00667
Macromolecules XXXX, XXX, XXX−XXX

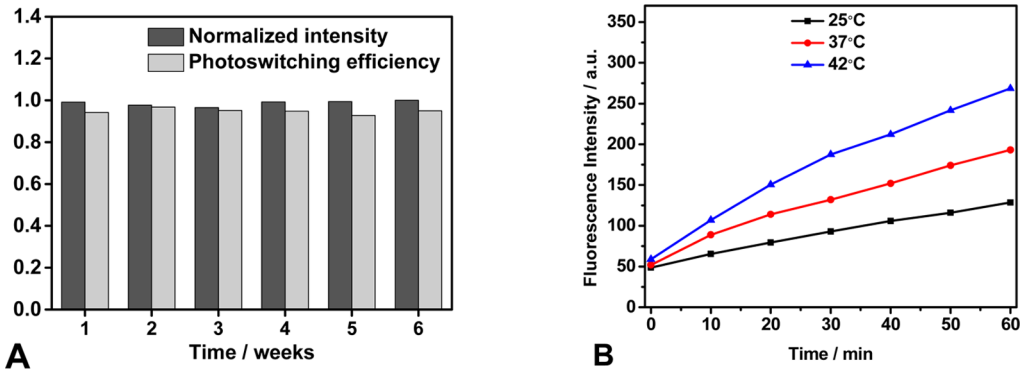

Figure 7. (A) Fluorescence long-term stability of PFPN sample (NP-N3, C_{PFPNs} = 0.3 wt %, λ_{ex} = 500 nm, λ_{em} = 550 nm). (B) Thermal stability of MC state in PFPNs dispersion (NP-N3, C_{PFPNs} = 0.3 wt %, λ_{ex} = 500 nm, λ_{em} = 550 nm) under physiological conditions (PBS, pH 7.4).

Presumably, it should be mainly attributed to the stable hydrophilic PEO shell and the protection of hydrophobic PMMA matrix as well as the covalent binding of dyes in the particles. The results demonstrated that the PFPNs could be used for long-term imaging or tracking in complex biological application. On the other hand, it is noteworthy that the ring-opened MC state of spiropyran units can return to the ring-closed SP state through the thermal isomerization pathway.[17] Thus, thermal stability of PFPNs sample (NP-N3) after UV irradiation at physiological conditions was investigated at three temperatures: 25, 37, and 42 °C. In contrast, as exhibited in Figure 7B, the fluorescence intensity of PFPNs sample at 550 nm recovered slowly at lower temperature, i.e., 25 °C, and it only added to 2.6-fold after being stored in the dark for 60 min, which was mainly attributed to the weak thermal isomerization of spiropyran moieties at room temperature. Therefore, the photoswitchable fluorescence property of PFPNs at room temperature should be more propitious to practical application.

Photorewritable Fluorescence Patterning. To take full advantage of the high contrast of photoswitchable fluorescence and favorable water-dispersibility nature, the prepared PFPNs aqueous dispersion (NP-N3) was used as luminescent paint for preparing photorewritable fluorescence patterning. The patterning on filter paper covered with PFPNs sample (NP-N3) was examined by modulated illumination through designed photomasks (Figure S10). As shown in Figure 8, the fluorescence pattern of letter "A" was recorded as a positive image upon 302 nm UV excitation by covering with mask A, which was subsequently erased by UV light. Then, another fluorescence patterning image of letter "B" was recorded upon 525 nm visible light excitation via covering with mask B (Figure 8) and then erased via illumination of visible light for ca. 20 min. The results indicated that the reversibly photoswitchable fluorescence property of PFPNs can be instantly used to fabricate photorewritable fluorescence patterning under the help of photomask.[18]

MTT Assay and Confocal Imaging of PFPNs in Living Cells. The cytotoxicity of PFPNs (NP-N3) was estimated via MTT assay by using A549 cells. For this test, the A549 cells were incubated with various concentrations of PFPNs for 24 h. The results in Figure 9 clearly indicate that no noticeable reduction in cell viability is observed for cells treated with PFPNs. It is noteworthy that over 85% of cell viability was reserved even at a high concentration of PFPNs (600 μg/mL), demonstrating that the PFPNs produced in this study is not obviously toxic *in vitro*.

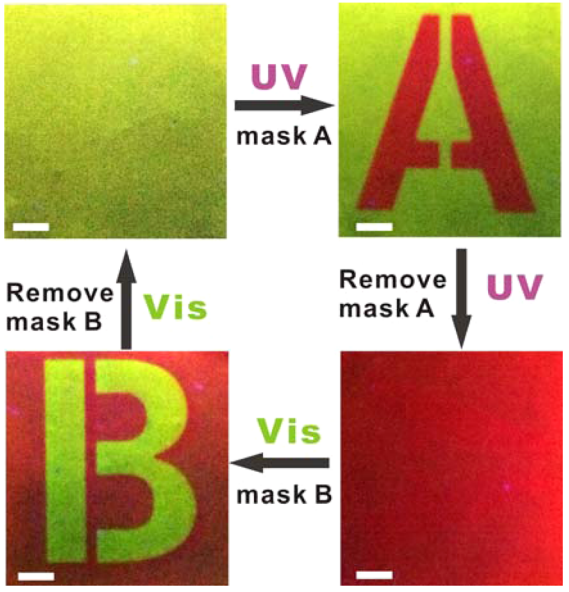

Figure 8. Photorewritable fluorescence patterning, prepared by PFPN dispersion (NP-N3), via using two photomasks (masks A and B, Figure S9) and irradiation of alternating 302 nm UV and 525 nm visible light. Scale bar: 1 cm.

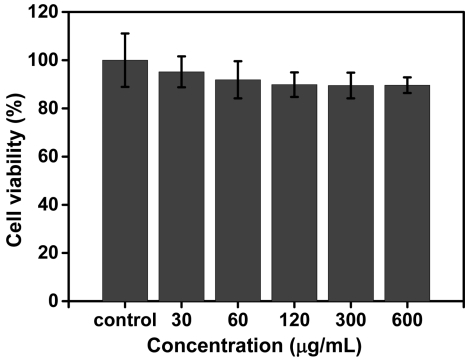

Figure 9. Cytotoxic effects of PFPNs sample (NP-N3) against A549 cells upon 24 h of incubation. Control: A549 cells in the absence of the PFPNs.

We also investigated the photoswitchable capability of the PFPNs in the living A549 (human lung carcinoma) cell lines (Figure 10). Under visible light irradiation, the green fluorescence from cells can be found as shown in Figure

DOI: 10.1021/acs.macromol.5b00667
Macromolecules XXXX, XXX, XXX−XXX

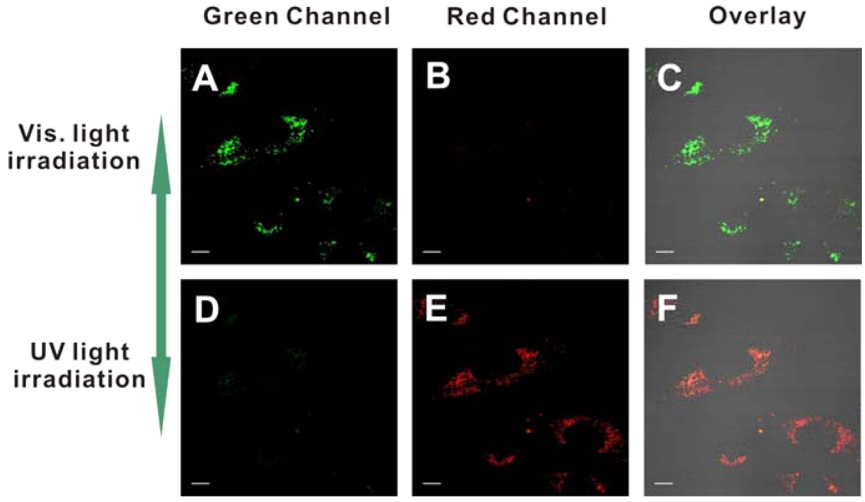

Figure 10. Confocal images of A549 cells treated with an amphiphilic PFPNs dispersion (NP-N3) at 37 °C for 3 h under visible light (A−C) or UV illumination (D−F). The overlay images confirm the signals are from nanoparticles in cell, not interference. Scale bar: 10 μm.

10A,C. It was mainly ascribed to the SPMA moieties in nanoparticles preserved as the nonfluorescence SP state, which cannot quench the fluorescence of BDPMA; therefore, the BDPMA in PFPNs emitted strong green fluorescence after excitation. After illumination of these A549 cells with UV light (30 s), the green fluorescence from cells has disappeared (Figure 10D), while the red fluorescence emitted from cells as exhibited in Figure 10E,F was clearly displayed. Because the SPMA moiety in nanoparticles has changed to its fluorescent MC state after irradiation of UV light, and the FRET process between MC state of SPMA and BDPMA occurred, which led to dramatic quenching of the green fluorescence of BDPMA (Figure 10D) and the remarkable appearance of the red fluorescence of the MC state of SPMA (Figure 10E). The results significantly demonstrated that the photoswitchable fluorescence property can also be realized in living cells, which revealed the potential advantage of PFPNs as smart fluorescent labels in complex biological environment with relatively high autofluorescence or another interfering fluorescence in the same wavelength region. Hence, the PFPNs may find broad applications in selectively highlighted complex biological systems with photoswitchable dual-color fluorescence.

CONCLUSIONS

In summary, novel amphiphilic BODIPY-based PFPNs have been successfully synthesized by a facile one-pot RAFT-mediated miniemulsion method, in which the macro-RAFT reagent was used both as reactive stabilizer and control agent. Meanwhile, the BDPMA dye and the photochromic SPMA can be covalently incorporated into the polymer backbone with controllable amount and ratio, which can significantly increase the structural stability and photostability of as-prepared PFPNs. Notably, the novel PFPNs displayed reversibly distinct dual-color (green-red) fluorescence not only in aqueous solution but also in the living cell by irradiation of UV or visible light via occurring switchable intraparticle FRET. In addition, the tunable FRET efficiency, prominent long-term stability, relatively fast photoresponsibility, and excellent photoreversibility together with their instantaneous application in rewritable fluorescence patterning further indicated that they are especially suited to applications in rewritable optical data storage and super-resolution biological imaging and labeling.

ASSOCIATED CONTENT

Supporting Information

Detailed description of synthesis of PEO-TTC, BODIPY phenol, and the amphiphilic polymeric nanoparticles; ^{1}H NMR spectrum of PEO-TTC, BODIPY phenol, BDPMA, and SPMA; detailed description of calculation of the R_0, E, r, and estimation of N_A, etc. The Supporting Information is available free of charge on the ACS Publications website at DOI: 10.1021/acs.macromol.5b00667.

AUTHOR INFORMATION

Corresponding Authors

*E-mail: cj0066@gmail.com (J.C.).
*E-mail: pgyi@hnust.cn (P.G.Y.).
*E-mail: jianhuijiang@hnu.edu.cn (J.H.J.).

Notes

The authors declare no competing financial interest.

ACKNOWLEDGMENTS

We gratefully acknowledge financial support of the present work by NSFC (Projects 51373002 and 21172066), Scientific Research Foundation for the Returned Overseas Chinese Scholars, Scientific Research Fund of Hunan Provincial Education Department (Project 12B041), Project funded by China Postdoctoral Science Foundation (Project 2014M550418), and Open Project Program of State Key Laboratory of Chemo/Biosensing and Chemometrics (Project 2013008).

REFERENCES

(1) (a) Tian, Z.; Wu, W.; Li, A. D. Q. *ChemPhysChem* **2009**, *10*, 2577−2591. (b) Tian, Z. Y.; Li, A. D. Q. *Acc. Chem. Res.* **2013**, *46*, 269−279. (c) Adam, V.; Mizuno, H.; Grichine, A.; Hotta, J. I.; Yamagata, Y.; Moeyaert, B.; Nienhaus, G. U.; Miyawaki, A.; Bourgeois, D.; Hofkens, J. *J. Biotechnol.* **2010**, *149*, 289−298. (d) Fries, K.; Samanta, S.; Orski, S.; Locklin, J. *Chem. Commun.* **2008**, 6288−6290. (e) Natali, M.; Soldi, L.; Giordani, S. *Tetrahedron* **2010**, *66*, 7612−7617.

(2) (a) Zhu, L.; Wu, W.; Zhu, M.-Q.; Han, J. J.; Hurst, J. K.; Li, A. D. Q. *J. Am. Chem. Soc.* **2007**, *129*, 3524−3526. (b) Zhu, M. Q.; Zhang, G. F.; Li, C.; Aldred, M. P.; Chang, E.; Drezek, R. A.; Li, A. D. Q. *J. Am. Chem. Soc.* **2011**, *133*, 365−372. (c) Wu, T.; Zou, G.; Hu, J. M.; Liu, S. Y. *Chem. Mater.* **2009**, *21*, 3788−3798. (d) Hu, Z.; Zhang, Q.;

DOI: 10.1021/acs.macromol.5b00667
Macromolecules XXXX, XXX, XXX−XXX

Xue, M.; Sheng, Q.; Liu, Y. *Opt. Mater.* **2008**, *30*, 851−856. (e) Wang, Y.; Hong, C. Y.; Pan, C. Y. *Biomacromolecules* **2012**, *13*, 2585−2593. (f) Chen, J.; Zeng, F.; Wu, S. Z.; Chen, Q. M.; Tong, Z. *Chem.—Eur. J.* **2008**, *14*, 4851−4860.

(3) (a) Feng, G. X.; Ding, D.; Li, K.; Liu, J.; Liu, B. *Nanoscale* **2014**, *6*, 4141−4147. (b) Wu, Y.; Xie, Y. S.; Zhang, Q.; Tian, H.; Zhu, W. H.; Li, A. D. Q. *Angew. Chem., Int. Ed.* **2014**, *53*, 2090−2094. (c) Pang, S. C.; Hyun, H.; Lee, S.; Jang, D.; Lee, M. J.; Kang, S. H.; Ahn, K. H. *Chem. Commun.* **2012**, *48*, 3745−3747. (d) Folling, J.; Polyakova, S.; Belov, V.; van Blaaderen, A.; Bossi, M. L.; Hell, S. W. *Small* **2008**, *4*, 134−142.

(4) (a) Lv, Y.; Liu, H.; Zhao, B. M.; Tian, Z. Y.; Li, A. D. Q. *Isr. J. Chem.* **2013**, *53*, 294−302. (b) Kong, L. C.; Wong, H. L.; Tam, A. Y. Y.; Lam, W. H.; Wu, L. X.; Yam, V. W. W. *ACS Appl. Mater. Interfaces* **2014**, *6*, 1550−1562. (c) Harbron, E. J.; Davis, C. M.; Campbell, J. K.; Allred, R. M.; Kovary, M. T.; Economou, N. J. *J. Phys. Chem. C* **2009**, *113*, 13707−13714.

(5) (a) Hell, S. W. *Science* **2007**, *316*, 1153−1158. (b) Michalet, X.; Pinaud, F. F.; Bentolila, L. A.; Tsay, J. M.; Doose, S.; Li, J. J.; Sundaresan, G.; Wu, A. M.; Gambhir, S. S.; Weiss, S. *Science* **2005**, *307*, 538−544. (c) Nienhaus, G. U. *Angew. Chem., Int. Ed.* **2012**, *51*, 1312−1314. (d) Tian, Z. Y.; Li, A. D. Q.; Hu, D. H. *Chem. Commun.* **2011**, *47*, 1258−1260. (e) Tian, Z. Y.; Wu, W. W.; Wan, W.; Li, A. D. Q. *J. Am. Chem. Soc.* **2011**, *133*, 16092−16100.

(6) (a) Diaz, S. A.; Menendez, G. O.; Etchehon, M. H.; Giordano, L.; Jovin, T. M.; Jares-Erijman, E. A. *ACS Nano* **2011**, *5*, 2795−2805. (b) Tomasulo, M.; Yildiz, I.; Raymo, F. M. *Aust. J. Chem.* **2006**, *59*, 175−178.

(7) (a) Li, C. H.; Zhang, Y. X.; Hu, J. M.; Cheng, J. J.; Liu, S. Y. *Angew. Chem., Int. Ed.* **2010**, *49*, 5120−5124. (b) Chen, J.; Zeng, F.; Wu, S.; Zhao, J.; Chen, Q.; Tong, Z. *Chem. Commun.* **2008**, 5580−5582.

(8) (a) Chen, J.; Zhang, P. S.; Fang, G.; Yi, P. G.; Zeng, F.; Wu, S. Z. *J. Phys. Chem. B* **2012**, *116*, 4354−4362. (b) Chen, J.; Zhang, P. S.; Fang, G.; Weng, C.; Hu, J.; Yi, P. G.; Yu, X. Y.; Li, X. F. *Polym. Chem.* **2012**, *3*, 685−693. (c) Chen, J.; Zeng, F.; Wu, S.; Su, J.; Tong, Z. *Small* **2009**, *5*, 970−978. (d) Chen, J.; Zhang, P. S.; Fang, G.; Yi, P. G.; Yu, X. Y.; Li, X. F.; Zeng, F.; Wu, S. Z. *J. Phys. Chem. B* **2011**, *115*, 3354−3362.

(9) (a) Derfus, A. M.; Chan, W. C. W.; Bhatia, S. N. *Nano Lett.* **2004**, *4*, 11−18. (b) Wang, L.; Wang, K. M.; Santra, S.; Zhao, X. J.; Hilliard, L. R.; Smith, J. E.; Wu, J. R.; Tan, W. H. *Anal. Chem.* **2006**, *78*, 646−654.

(10) (a) Li, W. W.; Min, K.; Matyjaszewski, K.; Stoffelbach, F.; Charleux, B. *Macromolecules* **2008**, *41*, 6387−6392. (b) Antonietti, M.; Landfester, K. *Prog. Polym. Sci.* **2002**, *27*, 689−757.

(11) (a) Rieger, J.; Stoffelbach, F.; Bui, C.; Alaimo, D.; Jerome, C.; Charleux, B. *Macromolecules* **2008**, *41*, 4065−4068. (b) dos Santos, A. M.; Le Bris, T.; Graillat, C.; D'Agosto, F.; Lansalot, M. *Macromolecules* **2009**, *42*, 946−956.

(12) Grazon, C.; Rieger, J.; Meallet-Renault, R.; Charleux, B.; Clavier, G. *Macromolecules* **2013**, *46*, 5167−5176.

(13) (a) Tomasulo, M.; Deniz, E.; Alvarado, R. J.; Raymo, F. M. *J. Phys. Chem. C* **2008**, *112*, 8038−8045. (b) Deniz, E.; Tomasulo, M.; DeFazio, R. A.; Watson, B. D.; Raymo, F. M. *Phys. Chem. Chem. Phys.* **2010**, *12*, 11630−11634.

(14) Ando, K.; Kawaguchi, H. *J. Colloid Interface Sci.* **2005**, *285*, 619−626.

(15) Liu, J.; Chew, C. H.; Gan, L. M.; Teo, W. K.; Gan, L. H. *Langmuir* **1997**, *13*, 4988−4994.

(16) Lakowicz, J. R. *Principles of Fluorescence Spectroscopy*; Kluwer Academic: New York, 1999.

(17) Tomasulo, M.; Deniz, E.; Alvarado, R. J.; Raymo, F. M. *J. Phys. Chem. C* **2008**, *112* (21), 8038−8045. Hammarson, M.; Nilsson, J. R.; Li, S. M.; Beke-Somfai, T.; Andreasson, J. *J. Phys. Chem. B* **2013**, *117* (43), 13561−13571.

(18) Li, C.; Yan, H.; Zhao, L.-X.; Zhang, G.-F.; Hu, Z.; Huang, Z.-L.; Zhu, M. Q. *Nat. Commun.* **2105**, DOI: 10.1038/ncomms6709.

DOI: 10.1021/acs.macromol.5b00667
Macromolecules XXXX, XXX, XXX−XXX